https://doi.org/10.5194/nhess-2020-92
Preprint. Discussion started: 8 April 2020

Natural Hazards and Earth System Sciences
Discussions

Tidal flood area mapping fronts the climate change scenarios: case study in a tropical estuary of Brazilian semiarid

Paulo Victor N. Araújo[1,2,3], Venerando E. Amaro[1,3], Leonlene S. Aguiar[3], Caio C. Lima[3,4], and Alexandre B. Lopes[5]

[1]Postgraduate Program in Geodynamics and Geophysics (PPGG), Federal University of Rio Grande do Norte, P.O. Box 1524, Natal-RN, 59078-970, Brazil
[2]Federal Institute of Education, Science and Technology of Rio Grande do Norte, Macau-RN, 59500-000, Brazil
[3]Laboratory of Geotechnologies, Coastal and Ocean Modelling (GNOMO), Department of Civil Engineering, Federal University of Rio Grande do Norte, Natal-RN, 59078-970, Brazil
[4]Federal Institute of Education, Science and Technology of Rio Grande do Norte, Natal-RN, 59015-000, Brazil
[5]Center of Sea Studies, Federal University of Parana, P.O. Box 61, Curitiba-PR, 83225-976, Brazil

Correspondence to: Paulo Victor N. Araújo (paulo.araujo@ifrn.edu.br)

Abstract. Previous studies on tidal flood mapping are mostly with continental and/or global scale approaches. Besides, the few works on local scale perception are concentrated in Europe, Asia, and North America. Here we present a case study approaching a flood risk mapping methodology against climate change scenarios in a region with a strong environmental and social appeal. The study site is an estuarine cut in the Brazilian semi-arid, covering part of two state conservation units, which has been in recent years suffering severe consequences from flooding by tides. In this case study, high geodetic precision data (LiDAR DEM), together with robust tidal return period statistics and data from current sea level rise scenarios were used. We found that approximately 118.26 km² of the estuary understudy is at high risk, extremely high risk and urgently in need of mitigation measures. This case study can serve as a basis for future management actions as well as a model for applying risk mapping in other coastal areas.

1 Introduction

Climate change has been associated with various environmental and socioeconomic damages worldwide, with global mean sea level rise (SLR) being one of the main associated phenomena (Nicholls and Cazenave, 2010; IPCC, 2014; Busman et al., 2016; Dangendorf et al., 2019; Bamber et al., 2019). During the last quarter-century, the global mean SLR has occurred at an accelerating rate, averaging about +3 mm/year, threatening coastal communities and ecosystems worldwide (Nerem et al., 2018; Bamber et al., 2019).

The changes produced by rising and falling the mean sea levels have important implications for the dynamics and morphology of coastal environments, and it is in these environments that a considerable part of the world's population lives (Neumann et al., 2015). Besides, it has been causing flooding of natural habitats and coastal infrastructures and consequently causing environmental and socioeconomic impacts of varying magnitude (Dwarakisha et al., 2009; IPCC, 2014; Murray et al., 2019).

Decades ago, the flooding usually happened only during a powerful or localized storm now can happen when a steady breeze or a change in coastal current overlaps with high tide (NOAA, 2019).
In Brazil, the current panorama of coastal flooding is extremely worrying (Losada et al., 2013). The Brazilian Panel on Climate Change (PBMC) systematized data and information indicating that the different regions of Brazil are already experiencing changes in their characteristic climates (PBMC, 2014). These changes are expected to affect the country's natural, human, infrastructure and production systems in a non-uniform manner (Brasil, 2016). The country stands out as the seventh largest nation in the world by coastal population and the seventh largest proportion of the coastal zone in the low-lying area (Mcgranahan et al., 2007). About 25% of the Brazilian population lives in the coastal zone and has lately been suffering from the damage caused by the relative rise in sea level (SMC-Brasil, 2018). Approximately 60% of the natural events that hit Brazil from 1948 to 2006 with harmful consequences to the population were related to flooding and/or sea advances (Brasil, 2016). These data, combined with scenarios of rising sea level trends (Easterling et al., 2000), warn of the need for (local scale) projections for the next decades, to support the preparation and planning to respond to increasing threat related to sea level rise. Climate risk adaptations involving large infrastructure investments represent difficult decisions and require an accurate information base (Hall et al., 2019; Kulp and Strauss, 2019).
Coastal flooding is becoming more frequent and expensive with sea level rise (SLR) (Herdman et al., 2018). The 5th report of the Intergovernmental Panel on Climate Change (IPCC) presented climate scenarios called Representative Concentration Pathway (RCP) (IPCC, 2014). Each RCP was built for the global scale and considers for the projection of relative elevation of MSL the historical evolution of several factors, such as gas emission, the concentration of effect gases, among others. Although in all scenarios the projected increase in MSL is a maximum of 1m for the year 2100, they have been prepared for global and continental scale. Many studies have analyzed the risk arising from these flood scenarios across the low-lying coastal zone (altitude up to 10m) (Nicholls et al., 2007; Dwarakish et al., 2009; Nicholls and Cazenave, 2010; Nicholls et al., 2011; Boori et al., 2012; Busman et al., 2016). However, the lack of work on the theme in focus in the South American region and especially in Brazil is striking. Therefore, the objective of this work was to carry out a tidal flood risk mapping, given the current scenarios of rising sea level trends, adopting as a case study the Piranhas-Açú Estuary, the northern portion of the state of Rio Grande do Norte, Brazil..

2 Study area

The tropical watershed of the Piancó-Piranhas-Açu River is located in northeastern Brazil and is the largest basin of the Northeast East Atlantic Hydrographic Region, with a total area of 43,683 km². Its territory is divided between the states of Paraíba (60%) and Rio Grande do Norte (40%). Fully inserted in very hot and semi-arid climate territory, the basin presents concentrated rainfall in a few months of the year (rainy late to autumn) and a pattern of strong interannual variability, characterized by alternation between years of above average, regular and consecutive years of below-average values resulting in prolonged droughts and low water availability. Like the other rivers in the basin, the Piancó-Piranhas-Açu river is an

https://doi.org/10.5194/nhess-2020-92
Preprint. Discussion started: 8 April 2020

intermittent river in natural conditions, and it rises in Serra de Piancó, in the state of Paraíba, and flows into the Atlantic Ocean on the northern coast of the state of Rio Grande do Norte, forming in its low course the Piranhas-Açu Estuary, is considered the most important river of the RN (Nascimento, 2009; ANA, 2016). Its perpetuation occurs through two regularization reservoirs built by the National Department of Drought Works (DNOCS): Curema/Mãe d'Água, in the State of Paraíba, and Armando Ribeiro Gonçalves, in the state of Rio Grande do Norte. These reservoirs correspond to the main water sources in the basin, which are also responsible for meeting external water demands, which are associated with adjacent basins. It should be noted that the basin will soon also be the recipient of water from the São Francisco River Basin Integration Project (SFIP). The study area covers the entire Piancó-Piranhas-Açú estuary. This area of approximately 536 km² is an estuarine section comprising parts of 4 municipalities of the northern coast of the state of Rio Grande do Norte (Porto do Mangue, Carnaubais, Pendencias, and Macau) (Figure 1).

This area is represented by a semi-arid climate, according to Nimer (Nimer, 1972), and it falls into the BSw'h category according to the Köppen classification (Köppen, 1948). The daily temperatures vary from 26°C to 30°C (with a mean temperature of 26.8°C), and the average relative air humidity is 70%. The pluviosity ranges from 1,300 to approximately 2,000 mm y-1 (IDEMA, 1999; Barbosa et al., 2018a). In geomorphological terms, there is a wide fluvial-marine plain that constitutes the Coastal Strip (Barbosa et al., 2018b, Costa et al., 2020). The number and extent of various channels present along adjacent large river plains reveal the great influence of oceanic waters on this stretch of the continent, with tidal action being one of the major natural forces responsible for hydrographic control.

In this region, the local tide is semidiurnal, with two high and two low tides, where the average level set as a reference is 1.39 m above the reduction level (RL), as established by the Hydrography and Navigation Directorate (DHN) of the Brazilian Navy. It has mean semidiurnal high tides of 2.34 m above reduction level, mean quadrature of high tides of 2.21 m, average low tide of 0.43 m of tidal seas below mean level of squared low seas of 0.56 m (Matos et al., 2019; DHN, 2018). As for the marine currents, the region is under the influence of the Southern Equatorial Current that acts throughout the northern coast of Brazil (Diniz et al, 2017).

In general terms, this coastal region has a mosaic of ecosystems marked by mangrove forests, exposed and sheltered sandy ocean beaches, barrier island systems and short-term high-sedimentary dynamic tidal channels (Grigio et al., 2006; Amaro et al., 2012; Santos and Amaro, 2013; Busman, et al., 2016). The industrial sector of the area understudy comprises essentially mineral exploration, especially salt, oil, and gas. The extraction of oil and natural gas is a very important activity in the basin and economy of the state of Rio Grande do Norte, due to the royalties generated (IDEMA, 2005). Aquaculture and artisanal fishing also play a part in the local economy, as well as irrigated agriculture, shrimp farming, salt marshes and, more recently, typical wind industry infrastructure.

There are two noteworthy state conservation units in the study area: Ponta do Tubarão State Sustainable Development Reserve (RDSEPT) and the Rosado Dunes Environmental Protection Area (APADR). RDSEPT was created through State Law No. 8.349 of July 18, 2003, and its objectives are to safeguard the traditional way of life, to ensure activities based on sustainable exploitation of natural resources, traditionally developed over generations and adapted. local ecological conditions and which

https://doi.org/10.5194/nhess-2020-92
Preprint. Discussion started: 8 April 2020

play a fundamental role in protecting nature and maintaining biological diversity. APADR was recently created by State Decree No. 27,695 of February 21, 2018, and aims to protect biological diversity, discipline the occupation process and ensure the sustainable use of the natural resources of the respective area.

Historically, although the Piranhas-Açú Estuary has suffered from some drastic river flooding in the last decade (2004, 2008 and 2009) as a result of extreme rainfall events (Medeiros and Zanella, 2019; Medeiros, 2019), it has been suffering lately with the effects of tidal flooding. Frequently, due to the effects of the sea, streets and houses are invaded by water, bringing negative consequences to several communities of the northern coast of Rio Grande do Norte (Figure 2). The current facts, allied to the local disordered occupation, the environmental and economic importance of the region, and, finally, the scenarios of sea level rise, make this region an area of great appeal for the development of scientific works, to subsidize information for decision-making on climate change adaptations.

3 Material and methods

Tidal flood risk mapping was performed using data on the meteorological tide, astronomical tide and a high-resolution LiDAR Digital Elevation Model (DEM), both calibrated for the study area. Data were subjected to statistical analysis and return period calculations. The 20-year return period was adopted as the base reference quota for this study and allied with the projections found in the literature on the global sea level rise for the coming years. Finally, flood risk mapping was performed based on flood scenarios and the vulnerability of land use and occupation.

3.1 Tide database

For this study, sea level variation was represented by the sum of the meteorological and astronomical tide (SMC-Brasil, 2018).

3.1.1 Meteorological tide (MT)

The MT or storm surge (also known as non-astronomical sea level) is the result of atmospheric forcing such as wind pressure or sea level pressure variations. To compose the local MT historical series, the maximum annual tide level was obtained from the data from point 19 (Lat. 4,821 ° W / Long. 36,500 ° S) (Figure 1) from the GOS (Global Ocean Surge) database of the SMC-Brasil project (SMC-Brasil, 2018). This database is a selection of regional reanalysis series, located along the Brazilian coast, built with a forced numerical simulation with atmospheric pressure fields and winds and validated for the region. Each of the series has a duration of 60 years (1948-2008) with a time interval of 1 hour (SMC-Brasil, 2018).

3.1.2 Astronomical tide (AT)

The AT is defined as the set of regular sea level rise and fall motions over 12 or 24 hours, produced by the gravitational effects of the Earth-Moon-Sun system. Other celestial bodies in the solar system are also attractive, yet small when compared to and considered by the moon and sun. Tide description and prediction at a given location can be done by harmonic tidal analysis

https://doi.org/10.5194/nhess-2020-92
Preprint. Discussion started: 8 April 2020

Natural Hazards and Earth System Sciences
Open Access
EGU
Discussions

(Pugh, 1987). For this study, the maximum annual astronomical tide level was used from the astronomical tide forecast data released by the Brazilian Navy's Directorate of Hydrography and Navigation (DHN), linked to the Port of Macau tidal gauge station (Lat. 4 ° 49 ' 05"S / Long 37 ° 02 '04" W) (Figure 1), during the period 1998 to 2018. These data were available through tables showing the maximum and minimum daily values of astronomical tidal heights.

3.1.3 Statistical analyses of tide database

The Mann–Kendall sequential test (Mann, 1945; Kendall, 1975) was applied to evaluate the temporal serial behavior of annual maximum of meteorological tide and astronomical tide. The Mann–Kendall test is a robust, sequential, and non-parametric statistical method used to determine if a specific data series has a temporal tendency towards statistically significant changes. Among its advantages, it does not require normal distribution of data and is only slightly influenced by abrupt changes or non-homogenous series (Zhang et al., 2009). In recent years, with growing concerns over environmental degradation and about the implications of greenhouse gases on the environment, researchers and practitioners have frequently applied the non-parametric Mann–Kendall test to detect trends in recorded hydrologic time series such as water quality, streamflow, and precipitation time series (Yue and Wang, 2004; Araújo et al., 2019). Although it has no influence on the tidal flood risk mapping, the Mann–Kendall test was applied to investigate if the elevation of tides is showing any upward or downward trend.

Then, the data was submitted for fit extreme value of gumbel distribution function (Gumbel, 1958). Extreme value statistics are used primarily to quantify the stochastic behavior of a process at unusually large (or small) values. Particularly, such analyses usually require estimation of the probability of events that are more extreme than any previously observed. Many fields have begun to use extreme value theory, and some have been using it for a very long-time including meteorology, hydrology, finance and ocean wave modeling to name just a few (Gilleland and Katz, 2016). The Gumbel Distribution also is known as Type I extreme value distribution, or Fisher-Tippet type I distribution, has the function of accumulated probabilities given by the equation, Eq. (1):

$$F_X(x) = P\{X < x\} = e^{-e^{-y}}, \tag{1}$$

Being *x* the ratio *y* a reduced variable Gumbel given by, Eq. (2):

$$y = \frac{x-\beta}{\alpha}, \tag{2}$$

Where α and β are characteristic parameters of the Gumbel line; α represents meter of scale and β the position parameter. The payback period (T*r*) in years can be obtained by the equation, Eq. (3):

$$x(Tr) = \beta - \alpha ln\left[-ln\left(1 - \frac{1}{Tr}\right)\right], \tag{3}$$

In this work, the 20-year return period (Tr20) was adopted as the starting reference for flood hazard mapping at present. All statistical analyses were performed using R software (R Development Core Team, 2020). The packages used were "Kendall" and "extRemes", for Mann – Kendall sequential test and fit extreme value of Gumbel distribution function, respectively.

3.2 Adjustment of Reduction Level to the Brazilian Geodetic System

The astronomical tidal information provided by DHN is all linked to the so-called Reduction Level (RL), which is the altimetric reference system for bathymetric depth measurement adopted by the Brazilian Navy (MB). This reference system assigns the average low tides of spring to a measurement reference made at the local level. Thus, the establishment of the local sea level found in the nautical charts and information provided by the Brazilian Navy has its own framework aimed at knowledge of the seabed relief for navigators' safety (CHM, 2019a, 2019b). Therefore, it is a different altimetric reference than the official geodetic reference system adopted by the country (Matos, 2005; Ramos & Krueger, 2009).

Therefore, to standardize the altimetric reference of this work, Imbituba's Datum Vertical was adopted, linked to the Brazilian Geodetic System (SGB). For this purpose, a level reference point was traced over approximately 50 minutes employing a two-frequency GNSS receiver (L1 / L2) near the port of Macau (Figure 3). This landmark, codenamed RN-2 (DHN), was deployed during the construction of the respective navigational station by the Brazilian Navy. After the screening, the GNSS data were submitted to coordinate adjustment post-processing to the MAPGEO2015 geoidal model and obtained its SGB-linked orthometric altitude, through the Precise Point Positioning of the Brazilian Institute of Geography and Statistics (IBGE-PPP). IBGE-PPP is a free online service for GNSS (Global Navigation Satellite System) data post-processing that makes use of the GPS Precise Point Positioning (CSRS) program developed by the Geodetic Survey Division of Natural Resources of Canada. It allows users with GPS and/or GLONASS receivers to obtain coordinates referenced to SIRGAS2000 (Geocentric Reference System for the Americas) and ITRF (International Terrestrial Reference Frame) through precise processing.

Finally, the reduction level (RL) orthometric altitude was obtained by mathematical subtraction operations at the RN-2 (DHN) level reference orthometric altitude, Eq. (4):

$$H(RL) = H(RN) - 4.046m = 2.92m - 4.046m = -1.126m, \quad (4)$$

3.3 LiDAR Digital Elevation Model

An airborne LiDAR DEM was used, with 1m horizontal spatial resolution and coverage for the entire local area. This DEM was built by PETROBRAS, granted in terms of technical cooperation between the said institution and the Federal University of Rio Grande do Norte (UFRN) and made available by the Graduate Program in Geodynamics and Geophysics (PPGG), utilizing a confidentiality agreement. The survey took place between February and September 2012, through integrated aero photogrammetry. In this aerial survey, a model ALS60 equipment manufactured by Leica Geosystems was used. The average point density was 4.2 per m², with a frequency of 200,000 pulses per second (200 kHz) and a 26 ° aperture angle (FOV). The operating frequency adopted was 160.2 kHz, with 65 Hz profiling frequency and an average aircraft speed of 190 km / h. The average point spacing was 0.41 m (in the flight direction) and 0.80 m in the transverse flight direction. The geodetic reference system adopted for planimetry was SIRGAS2000. For altimetry, the geoidal model MAPGEO2015 was used. The geometric altitude was converted to orthometric altitude to leave all in the same altimetric reference (All linked to the Brazilian Geodetic

https://doi.org/10.5194/nhess-2020-92
Preprint. Discussion started: 8 April 2020

Natural Hazards and Earth System Sciences
Open Access
EGU
Discussions

System). The altimetric RMSE of this product, obtained during the evaluation and calibration process (Araújo et al., 2018), was 0.1704 m.

3.4 Scenarios for mean sea level rise (MSL)

Sea level rise has been widespread in the international community as one of the impacts related to climate change, where most estimates are projected by the year 2100. For this work we adopted 3 scenarios of sea level rise at a global and regional level, to incorporate the predictions of average sea level rise until the year 2100. The forecast scenarios of the Intergovernmental Panel on Climate Change (IPCC) (RCP 4.5 = 0.53m and RCP 8.5 = 0.74m) (Church et al., 2013) and IBGE (ΔMLS = 2.1mm/year) (IBGE, 2016).

3.5 Tidal Flood Risk Mapping

For this work we adopted as a quantitative risk, the likelihood of harmful consequences or expected losses (dead, injured, destroyed and damaged buildings, etc.) occurring as a result of interactions between a natural hazard and conditions of local vulnerability (UNDP, 2004). The formula proposed by Wisner et al. (2011), where the same concept was one of the references of the fifth IPCC report (IPCC, 2014), Eq. (5):

$$Risk\ map = Hazard\ map\ X\ Vulnerability\ map, \tag{5}$$

Where, Hazard map is the likelihood of the process occurring with magnitude M (destructive potential) and Vulnerability map (physical vulnerability) is the degree of damage or loss to the exposed environment as a result of the impact and as a function of magnitude M.

For hazard mapping flooding was assigned 4 classes based on the scenarios understudy, in addition to the current flooding (Table 1). Each class represented the quota resulting from the sum of:

+ Projection of MSL elevation to 2100;
+ Meteorological tide (Tr20);
+ Astronomical tide linked to SGB (Tr20);
+ RMSE of DEM.

For the construction of the flood vulnerability mapping, the land use and occupation mapping of the region under study was first elaborated. The existing mapping in the literature, proposed by Lima (2016), was updated and expanded through the interpretation of the color image (RGB), vectoring the units in the 1:10,000 scale. Then, the land use and occupation mapping vector file were transformed into a raster file, with a spatial resolution of 1m, due to the spatial resolution of the altimetric data (DEM data). Finally, the raster file was reclassified with vulnerability values, in scores from 1 (least vulnerable) to 5 (most vulnerable), assigned to each use and coverage category (Table 2).

After obtaining the flood hazard and vulnerability maps, the risk map was obtained using the risk equation mentioned above. The risk was classified into 5 cassettes, according to the values in Table 3.

4 Results and discussion

The flood quota reached on a beach is a particularly complex phenomenon, both in the number of elements involved in the flooding process and in the interaction between these elements. However, it was possible to robustly model the complexity of tidal flooding that occurred in the Piranhas-Açú Estuary, as well as the risk in its probabilistic potential for the coming years.

4.1 Tidal behavior and return period

The effect of AT and MT on the coast is observed as a variation of sea level or free surface and it is at this level that waves propagate (SMC-Brasil, 2018). From the GOS data and DHN data applied in this work, it was possible to observe the tidal behavior in the tropical Piancó-Piranhas-Açu estuary (Figure 4).

The meteorological surge or storm surge is a sea level fluctuation caused by weather effects mainly derived from wind and variations in pressure fields. Throughout the 61 years of data from the GOS point, the maximum annual quota of the meteorological tide presented an average of 12cm and an amplitude of 14cm, with a maximum of 22cm and a minimum of 8cm, in the years 1964 and 1958, respectively. When applying the Mann-Kendall test, no statistically significant trend (Tau = -0.123; p= 0.16147) was observed in the dataset.

The astronomical tide is the result of the interaction of the gravitational forces of Earth, Moon and the Sun, being completely predictable. With the DHN data set provided by the Brazilian Navy, it was observed that the maximum annual astronomical tide quota presented an average of 2.80 m and a 13 cm amplitude, with a maximum of 2.84 m and a minimum of 2.71 m. In the same study, when the Mann-Kendall test was applied, no statistically significant trend was observed (Tau = 0; p= 1), showing a steady pattern.

The descriptive values on the tides presented to corroborate the values found in the literature. Frota et al. (2016), studying the tidal behavior in the Brazilian Northeast during the period from 2009 to 2011 in buoys about 200 km from the Piranhas-Açú estuary, found that the average maximum tide height was 2.79 m, ranging from 2.23 at 3.34 m. In the same study, Frota et al. (2016) found that the sea level variability in the sub-FT (The non-astronomical sea level signal) represents low oscillation, with a maximum of 0.12 m. Mattos et al. (2019), conducted a campaign from December 2010 to February 2011 to study significant wave heights, found that the tide table of Guamaré-RN (approximately 40km East of the table of Macau-RN) had averages of 2.34 m (in syzygy tides) and 2.21 m (in quadrature tides), both above the reduction level.

Regarding the return period (Tr20years), estimated by the Gumbel distribution function, the values of 15.90 cm and 2.90 m were found for MT and AT, respectively (Figure 5).

By performing the geodetic tracking of the DHN RN-2 framework, the ruler was adjusted to the Brazilian Geodetic System (SGB) and in this, the Reduction Level (RL) orthometric altitude, represented by the value of -1.126 m (Figure 3). Thus, the orthometric altitude of the maximum astronomical tide quota for the 20-year return period was 1.777 m, which served as a start for flood models.

4.2 Tidal flood hazard and vulnerability maps

It was possible to produce the four classes tidal flood hazard map for the study area based on the mean sea level projection values for the year 2100 (Table 5.4). In this product, the use of the astronomical tide quota linked to the Brazilian Geodetic System (SGB) was of paramount importance, thus ensuring that all input variables for flood hazard mapping were in the same geodetic framework.

After the spatialization of the classes in a GIS environment, the spatial behavior of the tidal flood hazard throughout the Piranhas-Açú estuary was verified (Figure 6a). In general, there was a positive north-south gradient, with a predominance of the flood class of the present scenario (high hazard). The high hazard class represented 257.60 km² of the estuary flood hazard, while the moderate hazard, low hazard, and extremely low hazard classes represented 286.26, 338.67 and 359.42 km², respectively.

Tidal flood stains were observed inside the urban area of the city of Macau. These spots are justified by the current layout of the city's drainage system, where at high tide times seawater enters the galleries and canals, affecting the interior of the city (Figure 6b and Figure 7). Aguiar et al. (2019) found the same structural problem in the urban area of Areia Branca city (approximately 58 km west of Macau city). It is important to mention that the land on which the local cemetery is in the urban area of Macau is one of the few urban sectors in the city not to suffer from tidal flood scenarios.

It was found that the flood event of January 3, 2015, had an orthometric altitude of 1.73m (Figure 8). The same spatial pattern of tidal flooding was observed between the photographic record and the flood model proposed in this work. Thus, validating the applied flood model.

By mapping the land use and land cover, it was obtained the quantification of the areas of the mapped units (Table 5.5 and Figure 9), highlighting the Caatinga area, which corresponded to 657.18 km².

Regarding the vulnerability map, it was observed that 66.86% (883.84km²) of the vulnerable areas had low flood vulnerability (Table 5.5 and Figure 10). However, it is important to note that 16% of vulnerable areas have High and Extremely High vulnerability, corresponding to an area of 205.30 km².

4.3 Tidal flood risk map

From the result of flood hazard and vulnerability mappings, the flood risk map was obtained (Figure 11).

The risk areas represent a total of approximately 360km², where the 135.23km² low-risk class stands out. While the other classes represented 85.64km² (extremely low risk), 20.25km² (moderate risk), 117.73km² (high risk) and 0.53km² (extremely high-risk). Extremely high-risk environments were sections of the urban areas of the cities of Porto do Mangue and Macau, and the communities of Ponta do Mel, Rosado and Diogo Lopes (Figure 10).

5 Conclusions

The rising of the sea level by a few millimeters per year is an important variable, as loss of land in lowland areas can quickly destroy coastal ecosystems such as lagoons, lagunas, and mangroves. In addition to flooding of socio-economically and environmentally sensitive and relevant areas, the rising sea levels can change the energy balance of coastal environments, causing large variations in the sedimentary process and consequently erosion of large stretches of the shoreline. (Castro et al., 2010). In the Piranhas-Açú Estuary, sea level rise was not statistically significant, we believe that the temporal scale of our meteorological tide data set (1948 to 2008) favored the masking of this phenomenon. Whereas, it has been noticeable by the local community and the news for the last 10 years only.

Possibly, tidal flooding in the region under study is closely linked to rising sea levels in recent years. Extreme tidal weather events are the main factor in flood danger. Flood hazard, vulnerability and risk maps are crucial for planning and intervention in flood prone areas. The case study results in the Piranhas-Açú Estuary can be used by local environmental management, mainly to characterize risk zones and to support the implementation of tidal flood risk management plans in this coastal area. The methodology and materials applied to this study area have proven to be effective in identifying tidal flood risk areas using high-resolution DEM that has been calibrated based on high precision GNSS, historical tidal quota data and geoprocessing techniques.

It is noteworthy that the methodological approach to the Piranhas-Açú Estuary is suitable to be replicated to other estuaries, particularly those in the Brazilian semiarid regions (estuaries with low hydrological contribution from rivers). Tidal flood risk mapping methodology may be particularly useful for regions with a good historical series of tide data. In this case study, the tide flood event modeling of 2015 was compared with the photographic records of the respective event and established high visual similarity between them.

This paper also demonstrates that well-applied geoprocessing techniques such as GIS and high precision geodesic provide results that can be very effective in environmental management with low-cost investments, highlighting the unique features of a given locality, especially floodplains and wetlands.

Conflicts of interest

None.

Acknowledgments

The authors express special thanks to the PETROBRAS for providing Digital Elevation Model LiDAR data. We also thank the reviewers of the Natural Hazards and Earth System Sciences (NHESS) journal for their many insightful comments.

References

Aguiar, L. S., Amaro, V. E., Araújo, P. V. N., and Santos, A. L. S.: Geotecnologias de Baixo Custo Aplicadas à Avaliação de Risco por Inundação em Áreas Urbanas Costeiras em Cenários de Mudanças Climáticas, Anuário do Instituto de Geociências – UFRJ, 42, 267-290, http://dx.doi.org/10.11137/2019_1_267_290, 2019.

Amaro, V. E.; Santos, M. S. T.; Souto, M. V. S.: Geotecnologias Aplicadas ao Monitoramento Costeiro: Sensoriamento Remoto e Geodésia de Precisão. 1ª Ed, Edição dos Autores, Natal, RN, 118 pp., 2012.

ANA - Agência Nacional das Águas: Plano de recursos hídricos da bacia hidrográfica do rio Piancó-Piranhas-Açu, Brasília-DF, 167 pp., available at: http://piranhasacu.ana.gov.br/produtos/PRH_PiancoPiranhasAcu_ResumoExecutivo_30062016.pdf (last access: 25 June 2019), 2016.

Araújo, P. V. N., Amaro, V. E.; Alcoforado, A. V. C., and Santos, A. L. S.: Acurácia Vertical e Calibração de Modelos Digitais de Elevação (MDEs) para a Bacia Hidrográfica Piranhas-Açú, Rio Grande do Norte, Brasil, Anuário do Instituto de Geociências – UFRJ, 41, 351–364, https://doi.org/10.11137/2018_1_351_364, 2018.

Araújo, P. V. N, Amaro, V. E., Silva, M. S. and Lopes, A. B.: Delimitation of flood areas based on a calibrated a DEM and geoprocessing: case study on the Uruguay River, Itaqui, southern Brazil, Natural Hazards and Earth System Sciences, 19, 237-250, https://doi.org/10.5194/nhess-19-237-2019, 2019.

Costa, L. R. F., Maia, R. P., Barreto, L. L., and Sales, V. C. C.: Geomorfologia do nordeste setentrional brasileiro: uma proposta de classificação, Revista Brasileira de Geomorfologia, 21, 185-208, http://dx.doi.org/10.20502/rbg.v21i1.1447, 2020.

Bamber, J. L., Oppenheimer, M., Kopp, R. E., Aspinall, W. P. and Cookeh, R. M.: Ice sheet contributions to future sea-level rise from structured expert judgment, Proceedings of the National Academy of Sciences, 116, 11195-11200, https://doi.org/10.1073/pnas.1817205116, 2019.

Barbosa, M. E. F., Boski, T., Bezerra, F. H. R., Gomes, M. P., Lima-Filho, F. P., Pereira, L. C., and Maia, R. P.: Late Quaternary infilling of the Assu River embayment and related sea level changes in NE Brazil, Marine Geology, 405, 23-37, https://doi.org/10.1016/j.margeo.2018.07.014, 2018a.

Barbosa, M. E. F., Bezerra, F. H. R., Boski, T., Lima-Filho, F. P., and Valdevino, D. S.: Padrões geomorfológicos na região estuarina do Rio Assu, NE – Brasil, Revista Brasileira de Geomorfologia, 19, 525-545, http://dx.doi.org/10.20502/rbg.v19i3.1208, 2018b.

Boori, M. S., Amaro, V. E. and Targino, A.: Coastal risk assessment and adaptation of the impact of sea-level rise, climate change and hazards: A RS and GIS based approach in Apodi-Mossoró estuary, Northeast Brazil, International Journal of Geomatics and Geosciences, 2, 815-832, 2012.

Brasil: Plano Nacional de Adaptação à Mudança do Clima, estratégias setoriais e temáticas, Ministério do Meio Ambiente, Brasília-DF, v.2, 295 pp., available at: https://www.mma.gov.br/images/arquivo/80182/LIVRO_PNA_Plano%20Nacional_V2_copy_copy.pdf (last access: 12 April 2019), 2016.

Busman, D. V., Amaro, V. E. and Souza-Filho, P. W. M.: Análise Estatística Multivariada de Métodos de Vulnerabilidade Física em Zonas Costeiras Tropicais. Revista Brasileira de Geomorfologia, 17, 499-516, http://dx.doi.org/10.20502/rbg.v17i3.912, 2016.

Castro, B. M., Brandini, F. P., Wainer, I. E. K. C. and Dottori, M.: O mar de amanhã, com as mudanças climáticas de hoje, Ciência e Cultura, 62, 40-42, available at: http://cienciaecultura.bvs.br/pdf/cic/v62n3/a16v62n3.pdf (last access: 11 November 2019), 2010.

CHM – Centro de Hidrografia da Marinha. Marinha do Brasil: Sondagem batimétrica, available at: https://www.marinha.mil.br/chm/dados-do-segnav-lev-hidro/sondagem-batimetrica (last access: 20 April 2019), 2019a.

CHM – Centro de Hidrografia da Marinha. Marinha do Brasil. Maregrafia e fluviometria. available at: https://www.marinha.mil.br/chm/dados-do-segnav-lev-hidro/maregrafia-e-fluviometria (last access: 20 April 2019), 2019b.

Costa, L. R. F., Maia, R. P., Barreto, L. L., and Sales, V. C. C.: Geomorfologia do nordeste setentrional brasileiro: uma proposta de classificação, Revista Brasileira de Geomorfologia, 21, 185-208, http://dx.doi.org/10.20502/rbg.v21i1.1447, 2020.

Dangendorf, S., Hay, C., Calafat, F. M., Marcos, M., Piecuch, C. G., Berk, K. and Jensen, J.: Persistent acceleration in global sea-level rise since the 1960s, Nature Climate Change, 9, 705-710, https://doi.org/10.1038/s41558-019-0531-8, 2019.

DHN - Diretoria de Hidrografia e Navegação: Tábuas de marés, available at: https://www.marinha.mil.br/chm/tabuas-de-mare (last access: 3 January 2018), 2018.

Diniz, C. H. G., Amaro, V. E., Prudêncio, M. C. and Felipe R. F.: Representação Tridimensional de Processos de Erosão Costeira em Ilhas Barreiras Utilizando Tecnologia de Jogos, Anuário do Instituto de Geociências – UFRJ, 40, 147-158, http://dx.doi.org/10.11137/2017_3_147_158, 2017.

Dwarakisha, G. S., Vinaya, S. A., Natesanb, U., Asanoc, T., Kakinumac, T., Venkataramanad, K., Paia, B. J. and Babitaa, M. K.: Coastal vulnerability assessment of the future sea level rise in Udupi coastal zone of Karnataka state, west coast of India, Ocean & Coastal Management, 52, 467-478, https://doi.org/10.1016/j.ocecoaman.2009.07.007, 2009.

Easterling, D. R., Meehl, G. A., Parmesan, C., Changnon, S. A., Karl, T. R. and Mearns, L. O.: Climate Extremes: Observations, Modeling, and Impacts, Science, 289, 2068–2074, http://dx.doi.org/10.1126/science.289.5487.2068, 2000.

Frota, F. F., Truccolo, E. C. and Schettini, C. A. F.: Tidal and sub-tidal sea level variability at the northern shelf of the Brazilian Northeast Region, Anais da Academia Brasileira de Ciências, 88, 1371-1386, http://dx.doi.org/10.1590/0001-3765201620150162, 2016.

Gilleland, E. and Katz, R. W.: extRemes 2.0: An Extreme Value Analysis Package in R, Journal of Statistical Software, 72, 1-39, http://dx.doi.org/10.18637/jss.v072.i08, 2016.

Grigio, A. M., Castro, A. F., Souto, M. V. S., Amaro, V. E., Vital, H. and Diodato, M. A.: Use of remoting sensing and geographical information system in the determination of the natural and environmental vulnerability of the Municipal District of Guamaré - Rio Grande do Norte - Northeast of Brazil, Journal of Coastal Research, Special Issue, 1427-1431, www.jstor.org/stable/25742990 (last access: 22 December 2019), 2006.

Gumbel, E. J.: Statistics of extremes. Columbia University Press, New York, 375 pp., 1958.

https://doi.org/10.5194/nhess-2020-92
Preprint. Discussion started: 8 April 2020

Natural Hazards and Earth System Sciences
Open Access
Discussions

Hall, J. W., Harvey, H. and Manning, L. J. Adaptation thresholds and pathways for tidal flood risk management in London, Climate Risk Management, 24, 42–58, https://doi.org/10.1016/j.crm.2019.04.001, 2019.

Herdman, L., Erikson, L. and Barnard, P.: Storm Surge Propagation and Flooding in Small Tidal Rivers during Events of Mixed Coastal and Fluvial Influence, Journal of Marine Science and Engineering, 6, 158, https://doi.org/10.3390/jmse6040158, 2018.

IBGE - Instituto Brasileiro de Geografia e Estatística: Análise do Nível Médio do Mar nas Estações da Rede Maregráfica Permanente para Geodésia – RMPG 2001/2015, Diretoria de Geociências, Coordenação de Geodésia, Rio de Janeiro, 65 pp., available at: ftp://geoftp.ibge.gov.br/informacoes_sobre_posicionamento_geodesico/rmpg/relatorio/relatorio_RMPG_2001_2015_GRRV.pdf (last access: 25 June 2019), 2016.

IDEMA - Instituto de Desenvolvimento Sustentável e Meio Ambiente: Informações dos municipios de Mossoró, Grossos e Tibau, v. 24, 1-24, 1999.

IDEMA - Instituto de Desenvolvimento Sustentável e Meio Ambiente: Projeto de Zoneamento Ecológico-Econômico dos Estuários do Rio Grande do Norte – ZEE/RN, Natal-RN, 35 pp., 2005.

IPCC: Climate Change 2014: Synthesis Report, Contribution of Working Groups I, II and III to the Fifth Assessment Report of the Intergovernmental Panel on Climate Change (IPCC), Geneva, Switzerland, 151 pp., 2014.

Kendall, M. G.: Rank Correlation Methods, Charles Griffin, London, 1975.

Köppen, W.: Klassifikation der Klimate nach Temperatur, Niederschlag und Jahreslauf, Petermanns Mitt, 64, 193-203, available at: http://koeppen-geiger.vu-wien.ac.at/pdf/Koppen_1918.pdf (last access: 01 June 2019), 1918.

Kulp, S. and Strauss, B. H.: New elevation data triple estimates of global vulnerability to sea-level rise and coastal flooding, Nature Communications, 10, 4844, https://doi.org/10.1038/s41467-019-12808-z, 2019.

Lima, C. C.: Sensoriamento remoto aplicado à atualização de informações geoambientais e ao estudo da dinâmica da paisagem no estuário do Rio Piranhas-Açu/NE do Brasil, Monographic, Geology degree, Federal University of Rio Grande do Norte, Natal, 141pp., http://dx.doi.org/10.13140/RG.2.2.26748.08326, 2016.

Losada, I. J, Reguero, B. G., Méndez, F. J., Castanedo, S., Abascal, A. J. and Mínguez, R.: Long-term changes in sea-level components in Latin America and the Caribbean, Global and Planetary Change, 104, 34–50, http://dx.doi.org/10.1016/j.gloplacha.2013.02.006, 2013.

Mann, H. B.: Nonparametric tests against trend, Econometrica, 13, 245–259, https://doi.org/10.2307/1907187, 1945.

Matos, M. F. A., Amaro, V. E., Scudelari, A. C. and Bezerra, A. C. N.: Análises estatísticas de alturas significativas de ondas de série temporal de curto prazo na costa do Rio Grande do Norte. Pesquisas em Geociências, 46, e0731, https://doi.org/10.22456/1807-9806.93246, 2019.

Matos, A. C. O. C.: Implementação de Modelos Digitais de Terreno para Aplicações na Área de Geodésia e Geofísica na América do Sul, Ph.D. theses, Postgraduate Program in Transport Engineering, Federal University of Sao Paulo, 335 pp., http://dx.doi.org/10.11606/T.3.2005.tde-10102005-104155, 2005.

McGranahan, G., Balk, D. and Anderson, B.: The rising tide: assessing the risks of climate change and human settlements in low elevation coastal zones, Environment and Urbanization, 19, 17–37, https://doi.org/10.1177%2F0956247807076960, 2007.

Medeiros, M. D.: Eventos hidroclimáticos extremos e vulnerabilidade socioambiental a inundações no Baixo-Açu – RN, Ph.D. theses, Postgraduate Program in Geography, Federal University of Ceara, Brazil, 209 pp., available at: http://www.repositorio.ufc.br/handle/riufc/35674 (last access: 22 December 2019), 2018.

Medeiros, M.D. and Zanella, M.E.: Estudo das vazões e estimativas de inundações no Baixo-Açu-RN, Geo UERJ, 40946, 1-30, http://dx.doi.org/10.12957/geouerj.2019.40946, 2019.

Murray, N. J., Phinn, S. R., DeWitt, M., Ferrari, R., Johnston, R., Lyons, M, B., Clinton, N., Thau, D. and Fuller, R. A.: The global distribution and trajectory of tidal flats, Nature, 565, 222-225, https://doi.org/10.1038/s41586-018-0805-8, 2019.

Nascimento, M. C.: A erosão costeira e sua influência sobre a atividade petrolífera: Alternativas sustentáveis na mitigação de impactos ambientais, MS Dissertation, Federal University of Rio Grande do Norte, Natal-RN, Brazil, 187 pp., available at: ftp://ftp.ufrn.br/pub/biblioteca/ext/bdtd/MiriamCN_DISSERT_1-100.pdf (last access: 14 September 2019), 2009.

Nerem, R. S., Beckley, B. D., Fasullo, J. T., Hamlington, B. D., Masters, D. and Mitchum, G. T.: Climate-change-driven accelerated sea-level rise detected in the altimeter era, Proc. Natl. Acad. Sci. U.S.A. 115, 2022–2025, https://doi.org/10.1073/pnas.1717312115, 2018.

Neumann, B., Vafeidis, A. T., Zimmermann, J. And Nicholls, R. J.: Future coastal population growth and exposure to sea-level rise and coastal flooding - a global assessment, PLOS ONE, 10, e0131375, https://doi.org/10.1371/journal.pone.0131375, 2015.

Nicholls, R. J. and Cazenave, A.: Sea-level rise and its impact on coastal zones, Science, 328, 1517-1520, http://dx.doi.org/10.1126/science.1185782, 2010.

Nicholls, R. J., Wong, P. P., Burkett, V., Codignotto, J., Hay, J., McLean, R., Ragoonaden, S., Woodroffe, C. D., Abuodha, P. A. O., Arblaster, J., Brown, B., Forbes, D., Hall, J., Kovats, S., Lowe, J., McInnes, K., Moser, S., Rupp-Armstrong, S. and Saito, Y.: Coastal systems and low-lying areas, in: Climate change 2007: impacts, adaptation and vulnerability. Contribution of Working Group II to the fourth assessment report of the Intergovernmental Panel on Climate Change, edited by: Parry, M. L., Canziani, O. F., Palutikof, J. P., van der Linden, P. J. and Hanson, C. E., Cambridge, UK, Cambridge University Press, 315-356, available at: http://ro.uow.edu.au/cgi/viewcontent.cgi?article=1192&context=scipapers (last access: 22 December 2019), 2007.

Nicholls, R. J., Hanson, S. E., Lowe, J. A., Warrick, R. A., Lu, X., Long, A. J. and Carter, T. R.: Constructing Sea-Level Scenarios for Impact and Adaptation Assessment of Coastal Areas: A Guidance Document. Technical Guidelines of the Task Group on Data and Scenario Support for Impact and Climate Analysis (TGICA) of the Intergovernmental Panel on Climate Change (IPCC), 64 pp., available at: https://www.ipcc-data.org/docs/Sea_Level_Scenario_Guidance_Oct2011.pdf (last access: 5 December 2019), 2011.

Nimer, E. Ensaio de um novo método de classificação climática: contribuição à climatologia intertropical e subtropical, especialmente do Brasil, Boletim de Geografia, Rio de Janeiro, 31, 141-153, 1972.

NOAA - National Oceanic and Atmospheric Administration: 2018 State of U.S. High Tide Flooding with a 2019 Outlook, NOAA Technical Report NOS CO-OPS 090, Silver Spring, Maryland, 31p., available at: https://repository.library.noaa.gov/view/noaa/20691 (last access: 9 November 2019), 2019.

PBMC - Painel Brasileiro de Mudanças Climáticas: Impactos, vulnerabilidades e adaptação às mudanças climáticas, Contribuição do Grupo de Trabalho 2 do Painel Brasileiro de Mudanças Climáticas ao Primeiro Relatório da Avaliação Nacional sobre Mudanças Climáticas, edited by: Assad, E.D. and Magalhães, A. R., COPPE, Federal University of Rio de Janeiro, Rio de Janeiro, RJ, Brazil, 414 pp., available at: http://www.pbmc.coppe.ufrj.br/documentos/RAN1_completo_vol2.pdf (last access: 10 October 2019), 2014.

Pugh, D. T.: Tides, surges and mean sea level: a handbook for Engineers and Scientists, John Wiley & Sons Ltd., New York, available at: https://eprints.soton.ac.uk/19157/1/sea-level.pdf (last access: 22 December 2019), 1987.

R Development Core Team: R: A language and environment for statistical computing, R Foundation for Statistical Computing, Vienna, Austria, available at: http://www.R-project.org/, last access: 28 February 2020.

Ramos, A. M. and Krueger, C. P.: Aplicação de reduções batimétricas GPS em levantamentos hidrográficos, Boletim de Ciencias Geodesicas, 15, 615–635, available at: https://revistas.ufpr.br/bcg/article/view/16284/10775 (last access: 22 December 2019), 2009.

Santos, M. S. T. and Amaro, V. E.: Dinâmica sazonal de processos costeiros e estuarinos em sistema de praias arenosas e ilhas barreira no nordeste do Brasil, Revista Brasileira de Geomorfologia, 14, 151-162, http://dx.doi.org/10.20502/rbg.v14i2.298, 2013.

SMC-Brasil: Níveis e cota de inundação, Documento temático, Ministério do Meio Ambiente, Brasília-DF, 130 pp., https://www.mma.gov.br/images/arquivo/80342/Livro_SMC_4___Niveis_e_Cota_de_inundacao.pdf (last access: 16 November 2019), 2018.

UNDP - United Nations Development Programme: Reducing Disaster Risk: A Challenge for development, A global report, 169 pp., available at: http://www.planat.ch/fileadmin/PLANAT/planat_pdf/alle_2012/2001-2005/Pelling__Maskrey_et_al_2004_-_Reducing_Disaster_Risk.pdf (last access 4 December 2019), 2004.

Wisner, B., Gaillard, J. C. and Kelman, I.: Framing disaster: theories and stories seeking to understand hazards, vulnerabilty and risk, in: The Routledge Handbook of Hazards and Disaster Risk Reduction, edited by: Wisner, B., Gaillard, J. C. and Kelman I., London, Routledge, 18-33, available at: https://www.routledgehandbooks.com/pdf/doi/10.4324/9780203844236.ch3 (last access: 7 November 2019), 2011.

Yue, S. and Wang, C.: The Mann–Kendall Test Modified by Effective Sample Size to Detect Trend in Serially Correlated Hydrological Series, Water Resour. Manage., 18, 201–218, https://doi.org/10.1023/B:WARM.0000043140.61082.60, 2004.

Zhang, W., Yan, Y., Zheng, J., Li, L., Dong, X., and Cai, H.: Temporal and spatial variability of annual extreme water level in the Pearl River Delta region, China, Global Planet. Change, 69, 35-47, https://doi.org/10.1016/j.gloplacha.2009.07.003, 2009.

https://doi.org/10.5194/nhess-2020-92
Preprint. Discussion started: 8 April 2020

Natural Hazards and Earth System Sciences
Open Access
Discussions

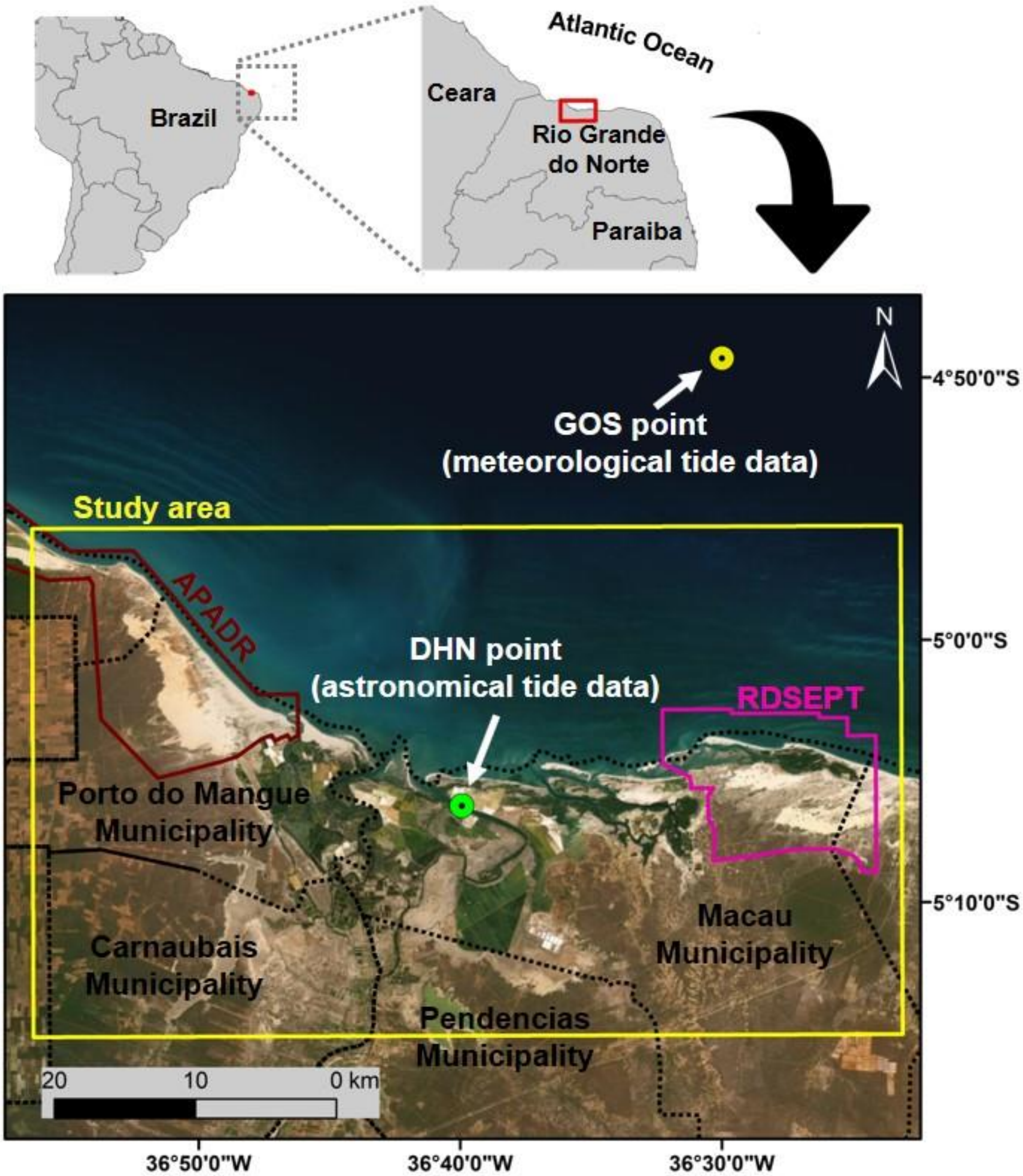

480 **Figure 1: Location of the study area. The yellow rectangle represents the delimitation of the study area: Pianco-Piranhas-Açu estuary and its surroundings. The pink polygon highlights the boundary of the Ponta do Tubarao State Sustainable Development Reserve (RDSEPT), while the burgundy polygon delimits the Rosado Dunes Environmental Preservation Area (APADR). Basemap from ArcGIS Online: © ESRI.**

https://doi.org/10.5194/nhess-2020-92
Preprint. Discussion started: 8 April 2020

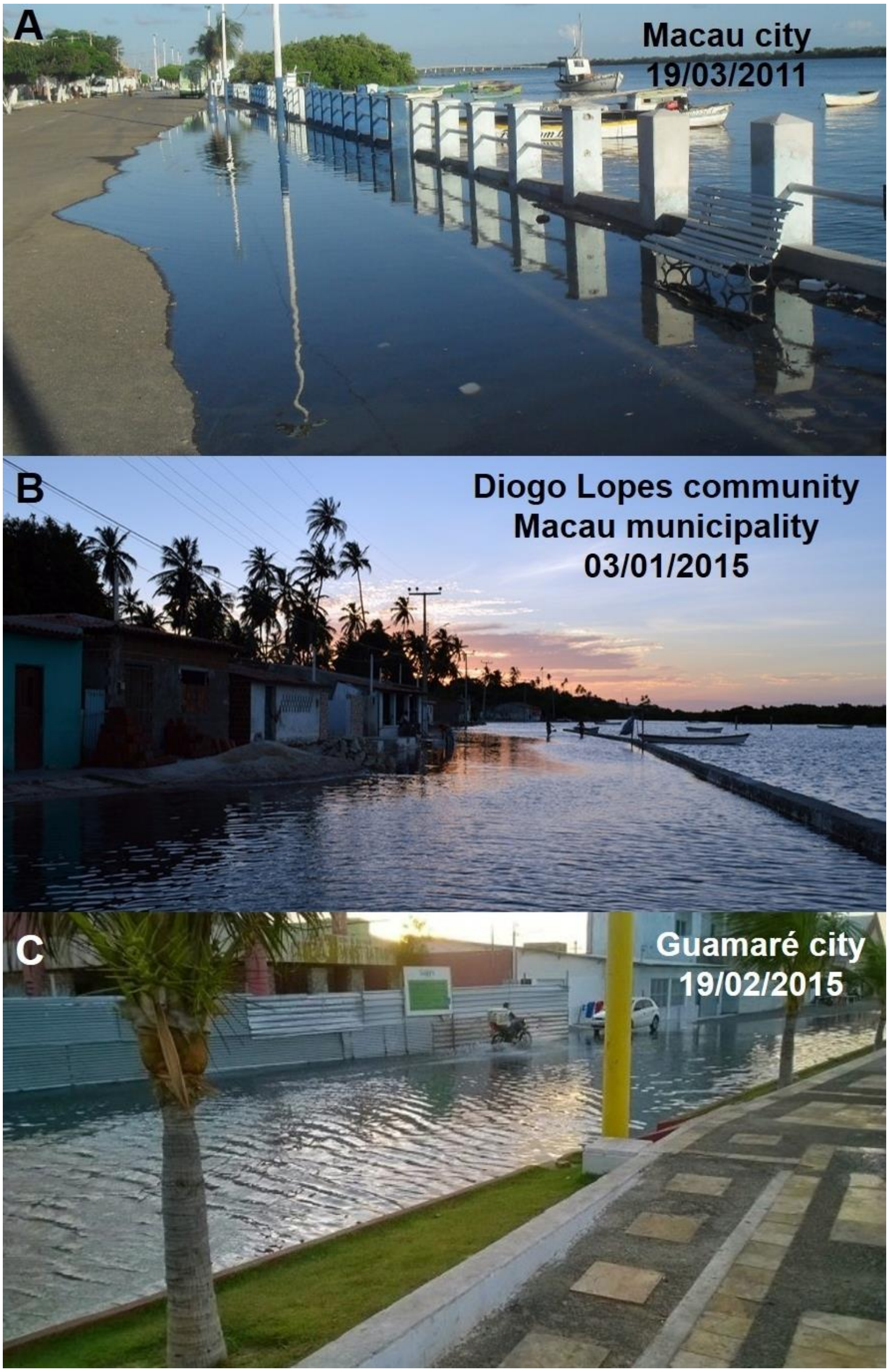

485 **Figure 2: Tidal flooding events in north coastal of Rio Grande do Norte State. (A) Macau urban area, Macau municipality, Mar 19, 2011 (Unknow author); (B) Diogo Lopes community, Macau municipality, Jan 03, 2015 (Tiago Ezequiel); and (C) Guamare urban area, Guamare municipality, Feb 19, 2015 (Unknown author).**

https://doi.org/10.5194/nhess-2020-92
Preprint. Discussion started: 8 April 2020

Natural Hazards and Earth System Sciences
Discussions

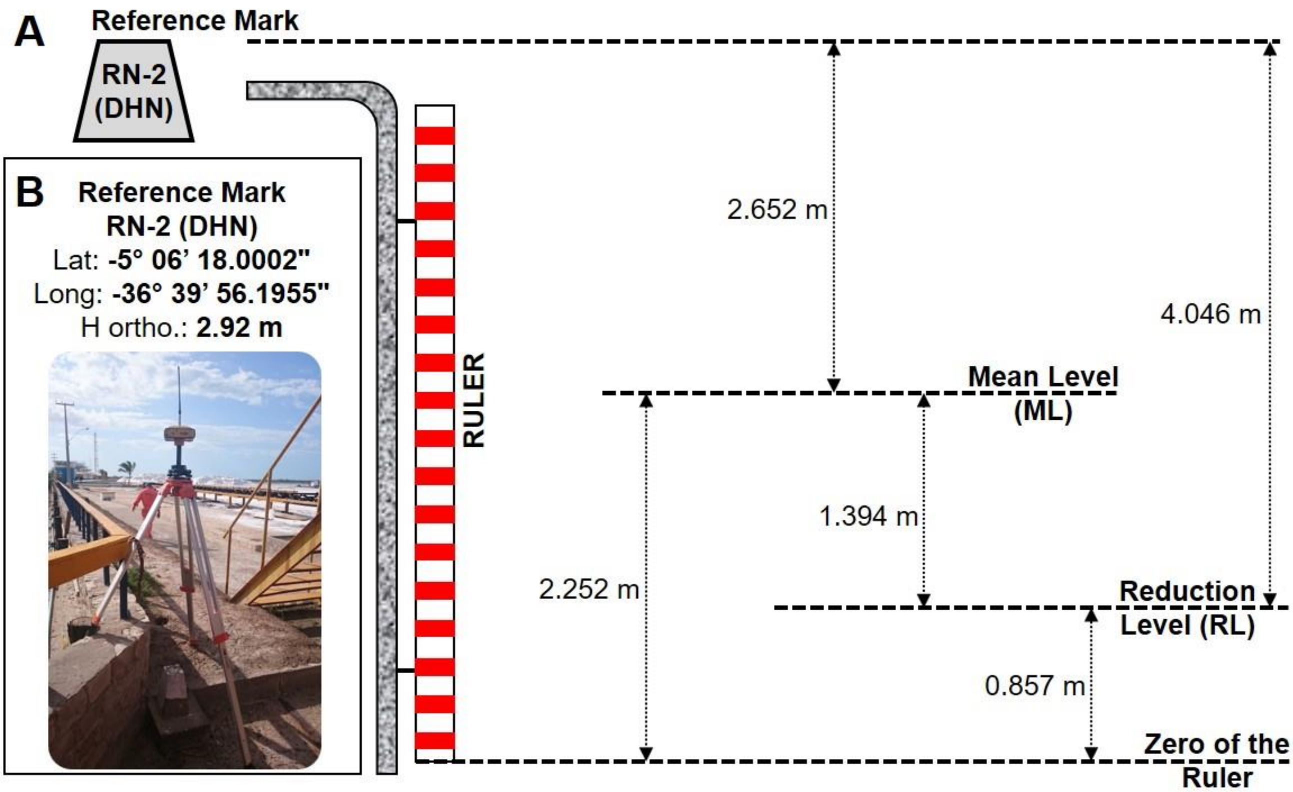

Figure 3: Scheme illustrating the differences in quotas between the references adopted by the Brazilian Navy: (A) Reference Mark RN-2 (DHN); and (B) Coordinates of Reference Mark RN2- (DHN).

https://doi.org/10.5194/nhess-2020-92
Preprint. Discussion started: 8 April 2020

Natural Hazards and Earth System Sciences
Discussions

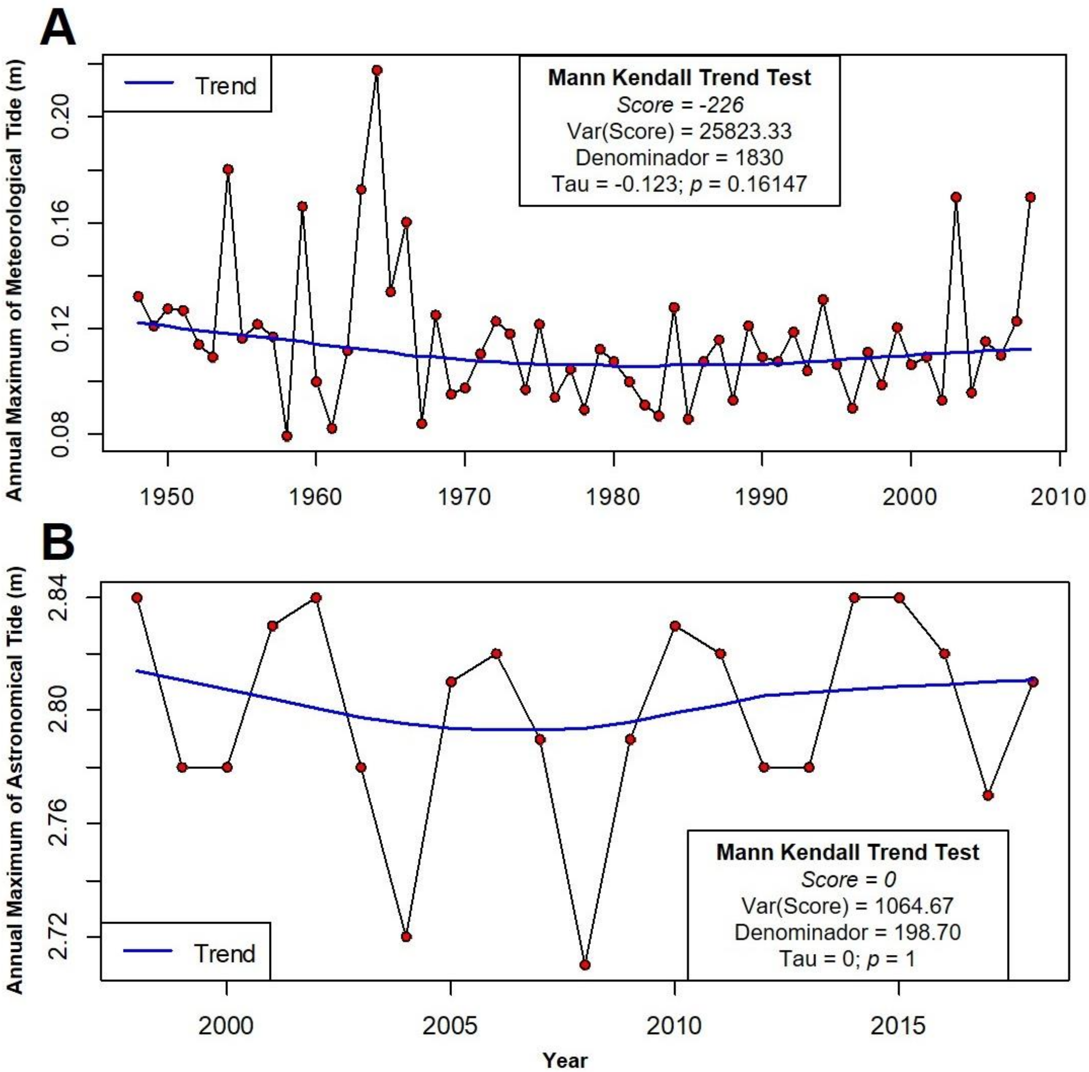

Figure 4: Annual tide maximum level temporal serie: (A) Meteorological tide; and (B) Astronomical tide.

515

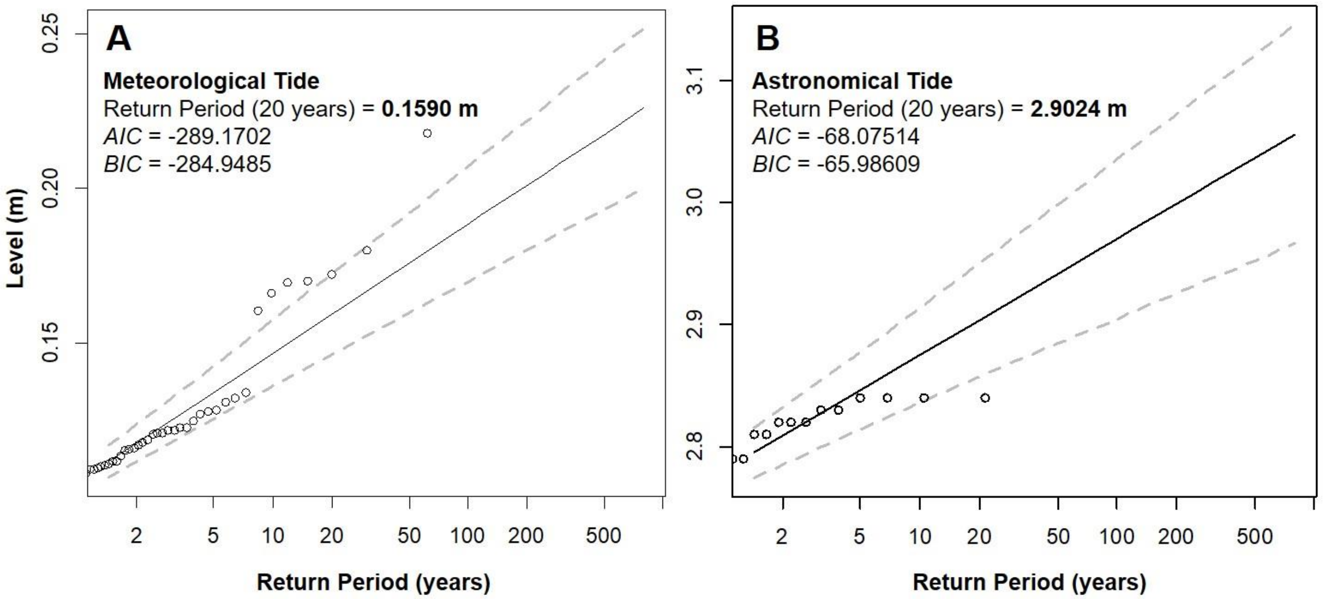

520

Figure 5: Return period graph of tide data: (A) Meteorological tide; and (B) Astronomical tide.

https://doi.org/10.5194/nhess-2020-92
Preprint. Discussion started: 8 April 2020

Natural Hazards and Earth System Sciences
Discussions

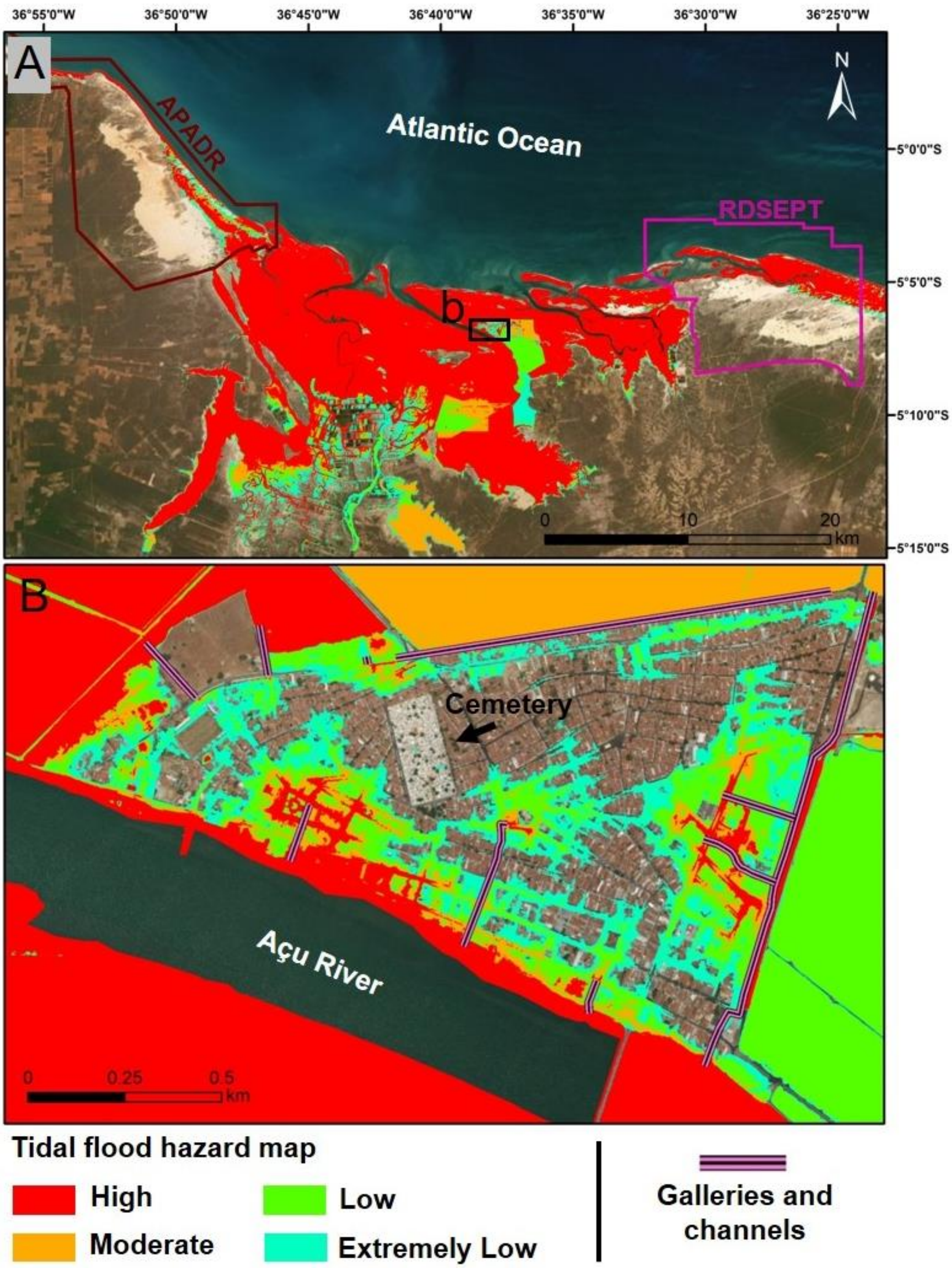

525 **Figure 6: Tidal flood hazard map: (A) Total area under study; and (B) Detail in Macau urban area. Basemap from ArcGIS Online: © ESRI.**

https://doi.org/10.5194/nhess-2020-92
Preprint. Discussion started: 8 April 2020

Natural Hazards and Earth System Sciences
Open Access
Discussions

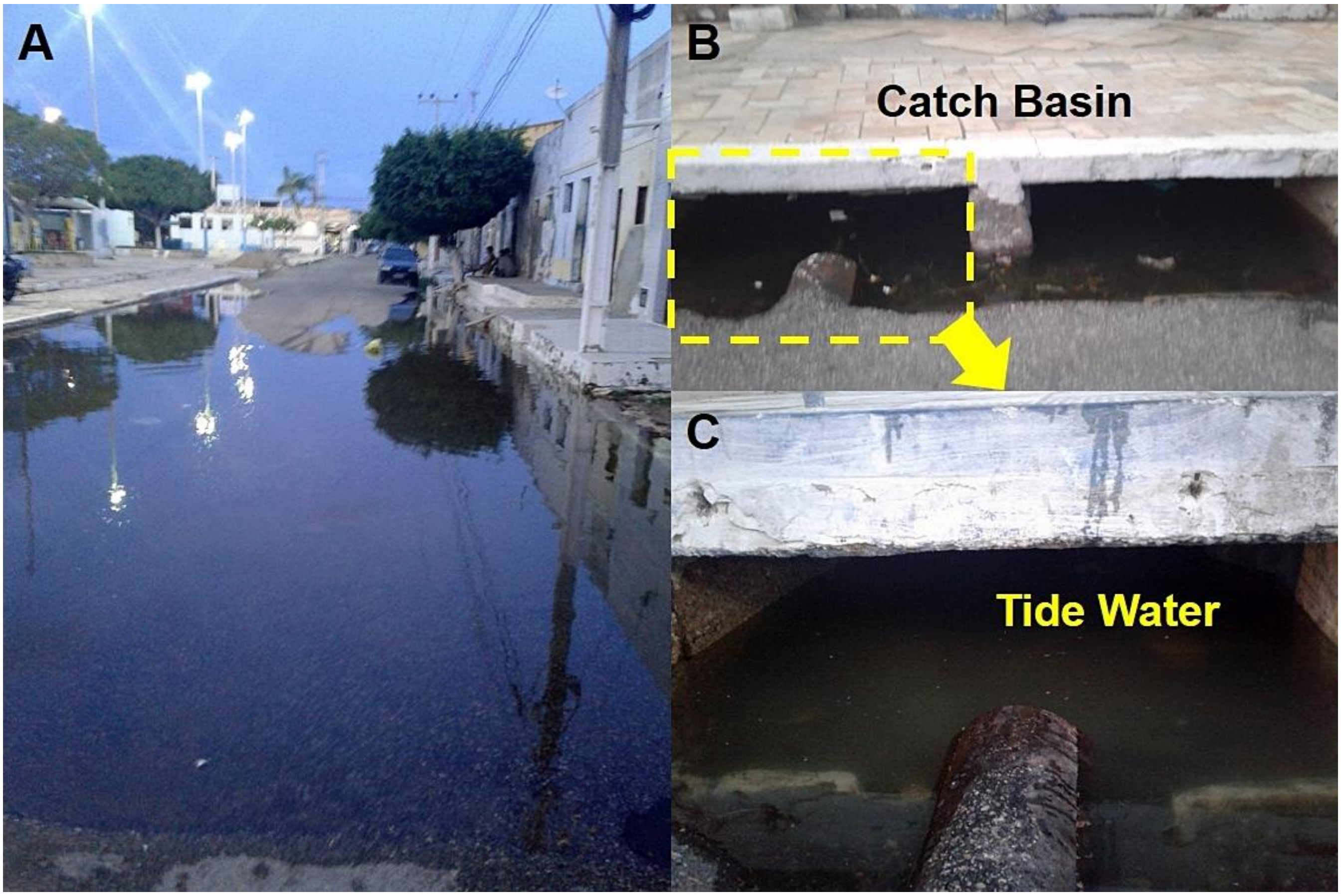

Figure 7: Tidal flood through the rain drainage system: (A) Tidal flooding event on March 10, 2020 (Macau urban area); (B) Example of local catch basin; and (C) Catch basin in detail.

https://doi.org/10.5194/nhess-2020-92
Preprint. Discussion started: 8 April 2020

Natural Hazards and Earth System Sciences
Open Access
Discussions

540

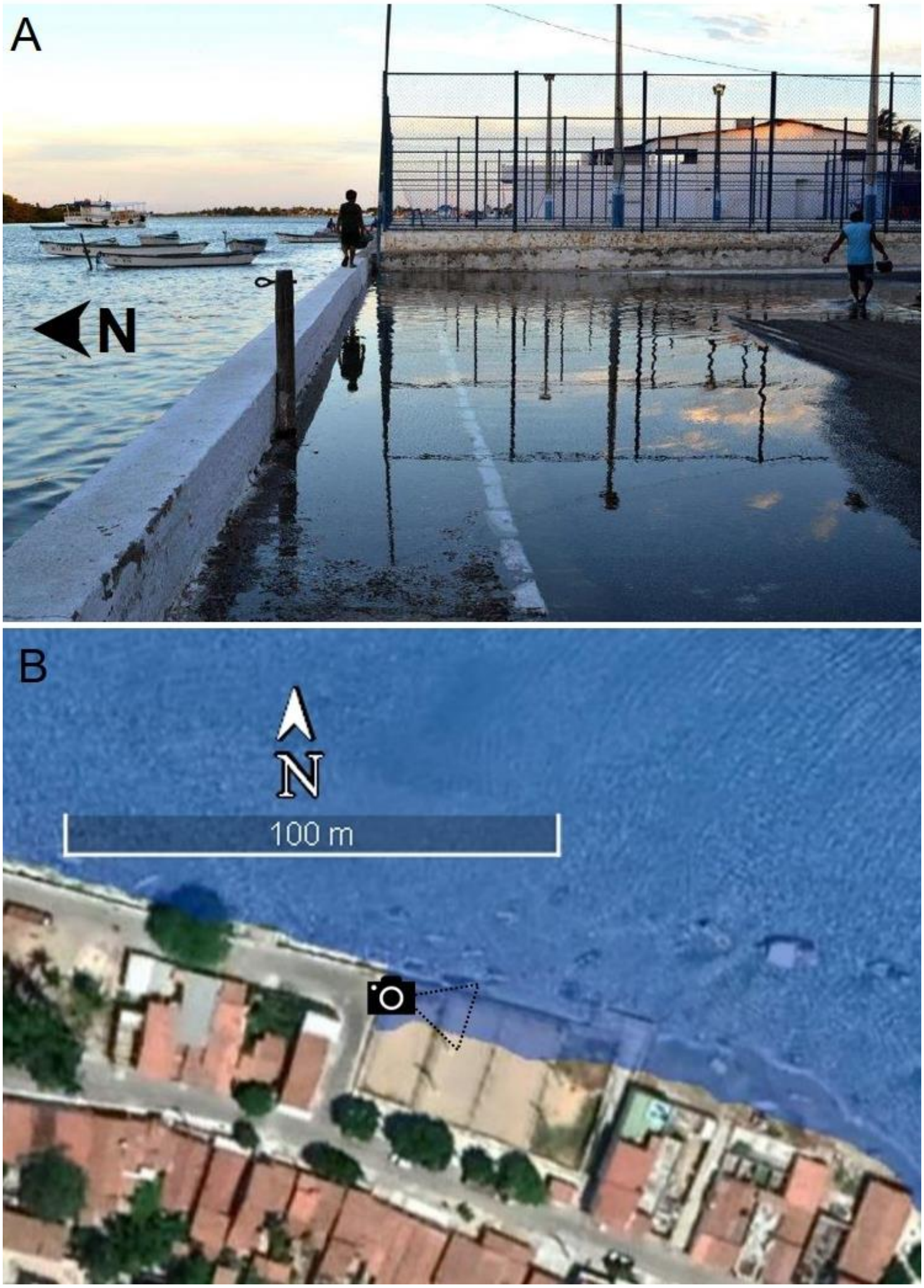

Figure 8: Tidal flooding events in north coastal of Rio Grande do Norte State: (A) Photographic record of Diogo Lopes community, Macau City, on January 3, 2015. (Tiago Ezequiel); and (B) simulated flood event for Diogo Lopes community on January 3, 2015. (orthometric height of tidal flood = 1.73m) (Basemap from Google Earth Pro: © Google LLC).

https://doi.org/10.5194/nhess-2020-92
Preprint. Discussion started: 8 April 2020

Natural Hazards and Earth System Sciences
Open Access
Discussions

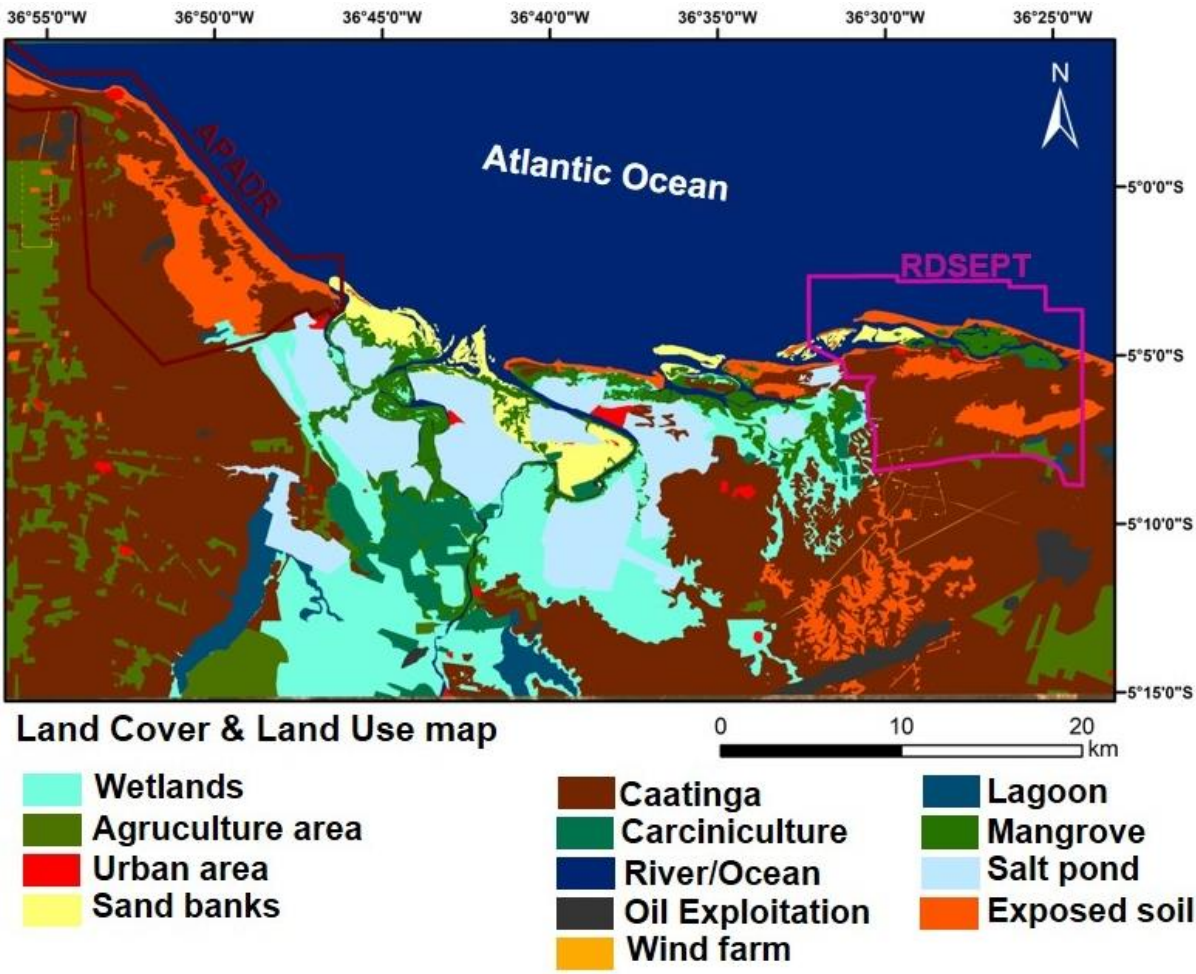

Figure 9: Land cover and land use map for study area.

https://doi.org/10.5194/nhess-2020-92
Preprint. Discussion started: 8 April 2020

560

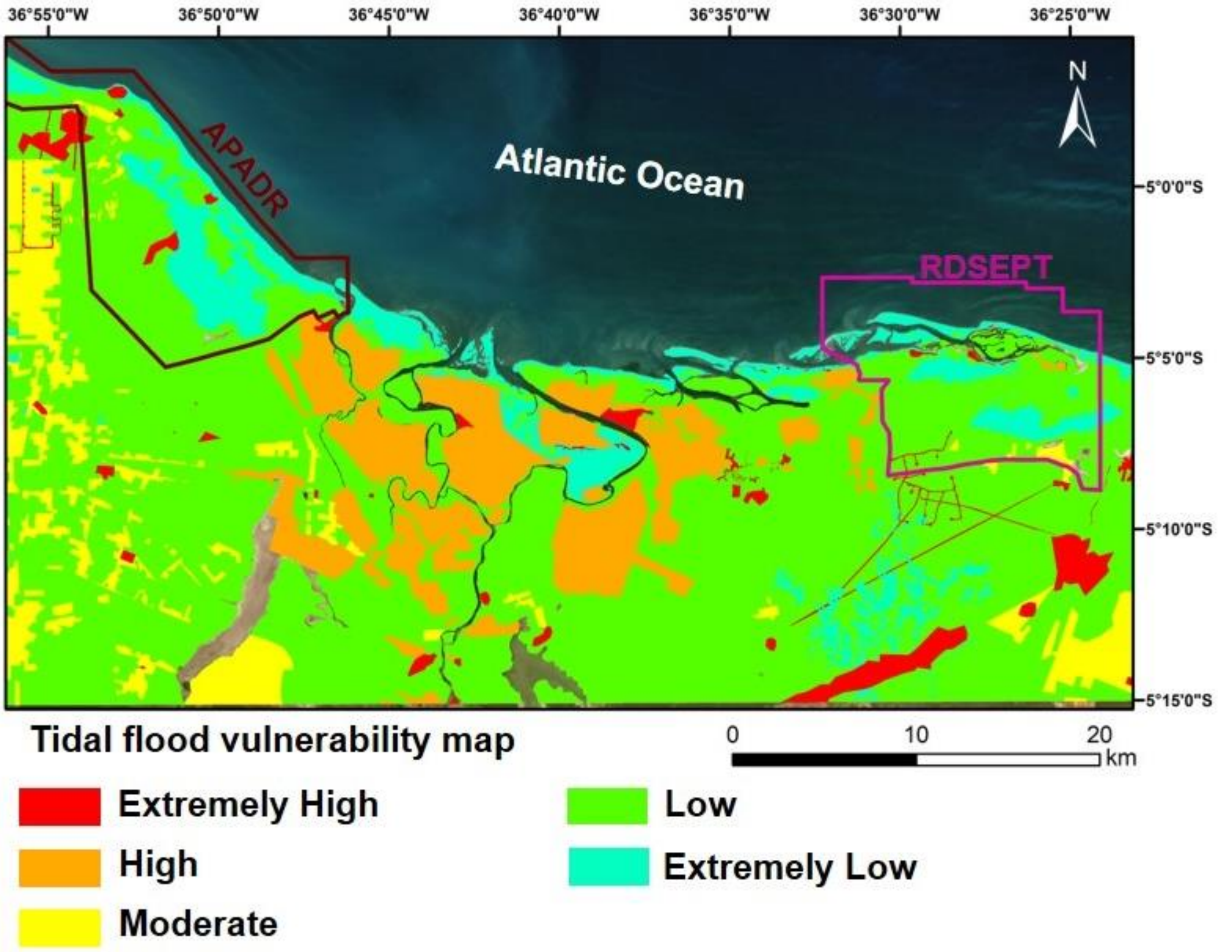

Figure 10: Tidal flood vulnerability map.

565

https://doi.org/10.5194/nhess-2020-92
Preprint. Discussion started: 8 April 2020

Natural Hazards and Earth System Sciences
Open Access
Discussions

570

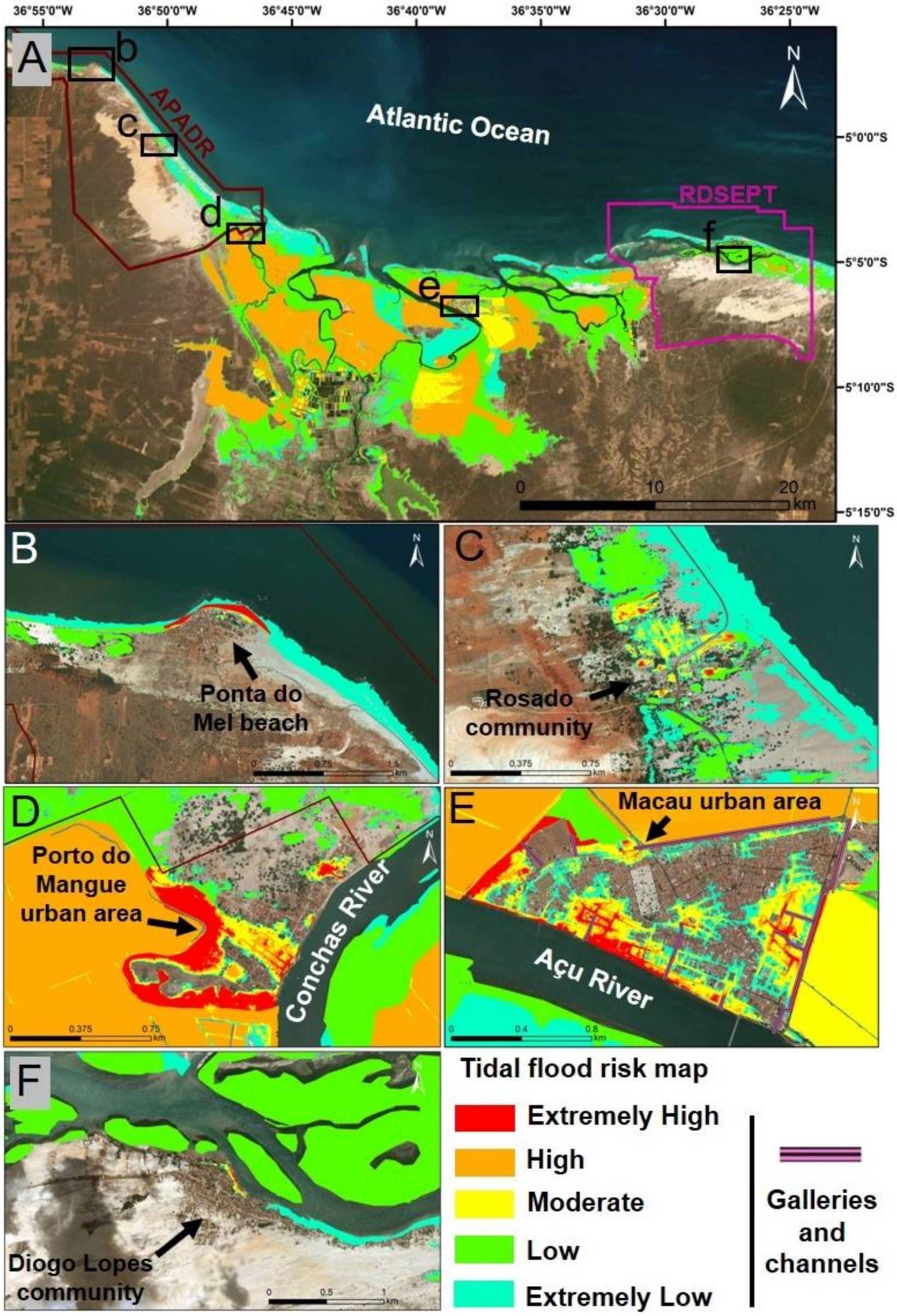

Figure 11: Tidal flood risk map for Piranhas Açu Estuary: (A) View of entire study area; (B) Ponta do Mel community; (C) Rosado community; (D) Porto do Mangue urban area; (E) Macau urban area; and (F) Diogo Lopes community. Basemap from ArcGIS Online: © ESRI.

https://doi.org/10.5194/nhess-2020-92
Preprint. Discussion started: 8 April 2020

Natural Hazards and Earth System Sciences
Discussions

Table 1: Attributed value to hazard map.

Scenario	Value	Hazard
Present	5	High
IBGE	4	Moderate
IPCC RCP 4.5	3	Low
IPCC RCP 8.5	1	Extremely Low

Table 2: Attributed value to vulnerability map.

Category	Value	Vulnerability
Urban area	5	Extremely High
Oil Explotation	5	Extremely High
Wind farm	5	Extremely High
Shrimp farm	4	High
Salt pond	4	High
Agriculture area	3	Moderate
Wetlands	2	Low
Caatinga	2	Low
Mangrove	2	Low
Sand banks	1	Extremely Low
Exposed soil	1	Extremely Low
Lagoon	0	No vulnerability
River/Ocean	0	No vulnerability

Table 3: Risk map value range.

Risk	Value Range
Extremely High	> 20 and ≤ 25
High	> 15 and ≤ 20
Moderate	> 10 and ≤ 15
Low	> 5 and ≤ 10
Extremely Low	> 0 and ≤ 5

https://doi.org/10.5194/nhess-2020-92
Preprint. Discussion started: 8 April 2020

Table 4: Tidal flood quotas in the scenarios under study.

Hazard Class	Projection of MSL elevation to 2100 (m)	Meteorological tide (Tr20) (m)	Astronomical tide linked to SGB (Tr20) (m)	RMSE of DEM (m)	Flood quota (m)
High	---	0.1590	1.7764	0.1704	**2.1058**
Moderate	0.1764	0.1590	1.7764	0.1704	**2.2822**
Low	0.5300	0.1590	1.7764	0.1704	**2.6358**
Extremely Low	0.7400	0.1590	1.7764	0.1704	**2.8458**

Table 5: Area of land cover and land use categories.

Category	Area (km²)	Vulnerability	Area (km²)
Urban area	7.84	Extremely High	40.17
Oil Explotation	27.37		
Wind farm	4.96		
Shrimp farm	34.19	High	165.13
Salt pond	130.94		
Agriculture area	115.10	Moderate	115.10
Wetlands	174.74	Low	883.84
Caatinga	657.18		
Mangrove	51.91		
Sand banks	29.86	Extremely Low	117.61
Exposed soil	87.75		
Lagoon	24.22	No vulnerability	873.20
River/Ocean	848.97		